International Statistical Review (1991), **59**, 2, pp. 139–161. Printed in Great Britain

Some Statistical Features of the Long-Term Variation of the Global and Regional Seismic Activity

Yosihiko Ogata[1] **and Katsuyuki Abe**[2]

[1]Institute of Statistical Mathematics, 4-6-7 Minami-Azabu, Tokyo, Japan 106. [2]Earthquake Research Institute, University of Tokyo, Tokyo, Japan

Summary

The temporal variation of the shallow earthquake activity of the entire world and the regional area around Japan is statistically investigated on the basis of two catalogs of earthquakes: one is Abe's catalog for global earthquakes with magnitude $M_S \geqslant 7$ in the period 1897 through 1980, and the other is Utsu's catalog for the earthquakes in and around Japan with magnitude $M_J \geqslant 6$ in the period 1885 through 1980. The occurrence rate of earthquakes in both the areas is high in the period from 1920's through 1940's and low in the last 30 years. This persistent fluctuation or trend in appearance can be related to a long-range statistical dependence of the time series of earthquake occurrence. Indices measuring the strength of such dependence are calculated for each catalog to compare with statistical models. Although Pérez & Scholz (1984) have claimed the inhomogeneity of the earthquake catalogs under the postulate of constant rate of earthquake occurrence for the world through the century, their rationale is not always guaranteed in view of the long-range dependence nature of earthquake occurrence. The synchronous variation of seismic frequency in the high latitude area of the world and in the regional area around Japan obtained from the independent catalogs is suggestive of an external effect such as a large-scale motion of the earth rather than the presupposed inhomogeneity of the catalogs.

Key words: Dispersion-time diagram; Heterogeneity and homogeneity of earthquake catalog; Long range dependence; Magnitude; $1/f$-spectrum; Point processes; R/S-statistics; Self-similarity; Simulations; World's and Japan's seismic activities of this century; Z-test

1 Introduction

A heterogeneity of existing earthquake catalogs has been the fundamental problem in seismology. In recent years, Pérez & Scholz (1984) applied the normal deviate (Z) test to an identification of proposed rate change in the world seismicity and claimed that two remarkable changes in the rate around 1922 and 1948 resulted from inhomogeneity of earthquake catalogs for instrumental-related reasons. It is obvious that their claim strongly depends on their a priori assumption of an independent or short-range dependence of earthquake occurrence. This assumption can be criticized from the viewpoint of long-range dependence of seismicity. It is well known in statistical studies that various records in geophysics really exhibit self-similarity. Our naive interest therefore is led to examine whether the time series of earthquake occurrence possesses the nature of the short-range or long-range dependence. We make some statistical analyses of spectrum, dispersion-time diagrams and R/S for estimating and testing of the point process data. The major purpose of this paper is to investigate the seismic activity by the statistical means and to discuss against the presupposed inhomogeneity of earthquake catalogs. We use two catalogs for the entire world and the regional area around Japan. Both the catalogs cover a period of about 100 years. We also attempt to show the possibility that the apparent rate change in the global seismicity can be simulated by a certain long-range correlated process.

2 Data

In this study, two sets of a catalog of shallow earthquakes are used for discussing the temporal pattern of the seismicity. One is the catalog of global earthquakes, and the other is the catalog of regional earthquakes that occurred in and around Japan. Abe (1981) prepared a revised magnitude catalog of global earthquakes for the period 1904–1980. This catalog lists the surface-wave magnitude M_S of every reported large event, according to the original formulation of Gutenberg (1945). Later, Abe & Noguchi (1983a, b) added earthquakes that occurred in the early period 1897–1917. Some corrections were complemented later by Abe (1984). These catalogs give a highly complete list of large shallow earthquakes for the period 1897–1980 (magnitude $M_S \geq 7$, depth $\leq$70 km or shallow depth) on a uniform basis. All these catalogs are mutually consistent in use of the magnitude scale and hereafter called collectively Abe's catalog.

A similar catalog of earthquakes in and around Japan was prepared by Utsu (1982b). The magnitude scale M_J used there is entirely based on the definition of Tsuboi (1954). The scale is close to M_S but there is a systematic deviation (Utsu, 1982c). On average, M_J differs from M_S by 0·23 units at $M_J = 6{\cdot}0$ and $-0{\cdot}30$ units at $M_J = 8{\cdot}0$ (Hayashi & Abe, 1984). The magnitudes of earthquakes for the period 1926–1980 are given by the Seismological Bulletins of Japan Meteorological Agency, and the magnitudes for the period 1885–1925 are determined by Utsu (1979, 1982a). Utsu (1982b) compiled these catalogs into one complete catalog for the period 1885–1980. Its catalog for shallow earthquakes (magnitude $M_J \geq 6$, depth $\leq$60 km or shallow depth) in the Region A of Utsu (1982b) is hereafter called Utsu's catalog.

Figure 1(a) shows the cumulative number of shocks with $M_S \geq 7$ from the Abe's world catalog. The general trend seems to be approximated by three straight lines, the middle part being steeper than the other parts. A similar graph was the motive point of Pérez & Scholz (1984). They assumed that the seismic rate should be constant throughout the century and concluded that the apparent high rate in the middle part from 1922 through 1948 is due to the biased magnitude estimation. Here we check the detail of the seismicity rates in two divided areas of the world: one is low latitude area between 20°N and 20°S, and the other is high latitude area of northward of 20°N and southward of 20°S. If the apparent high rate resulted from the systematic magnitude shift by the instrumentally-related reasons as Pérez & Scholz claimed, we should have the similar cumulative lines in the two areas. However, Figs. 1(c) and 1(d), displaying the cumulative number in the two areas, clearly show the regional difference in the changing seismicity rate. Neither of the two seems to be approximated by three straight lines. The trend of respective lines is stable in the sense that each of the two cumulative lines does not change much by the choice of the boundary latitude: for instance, 30° instead of 20°. The similar and very clear difference of regional activity is demonstrated by Mogi (1979) for very large earthquakes with $M \geq 7{\cdot}8$.

The very similar trend in the cumulative lines is shown in Fig. 1(d) for the high latitude area from the Abe's catalog and in Fig. 1(b) for the region around Japan with $M_J \geq 6$ from the Utsu's catalog. It is shown in these figures that the frequency rates are high in the period 1920's to 1940 and are gradually decreasing in the last 30 years. The decreasing

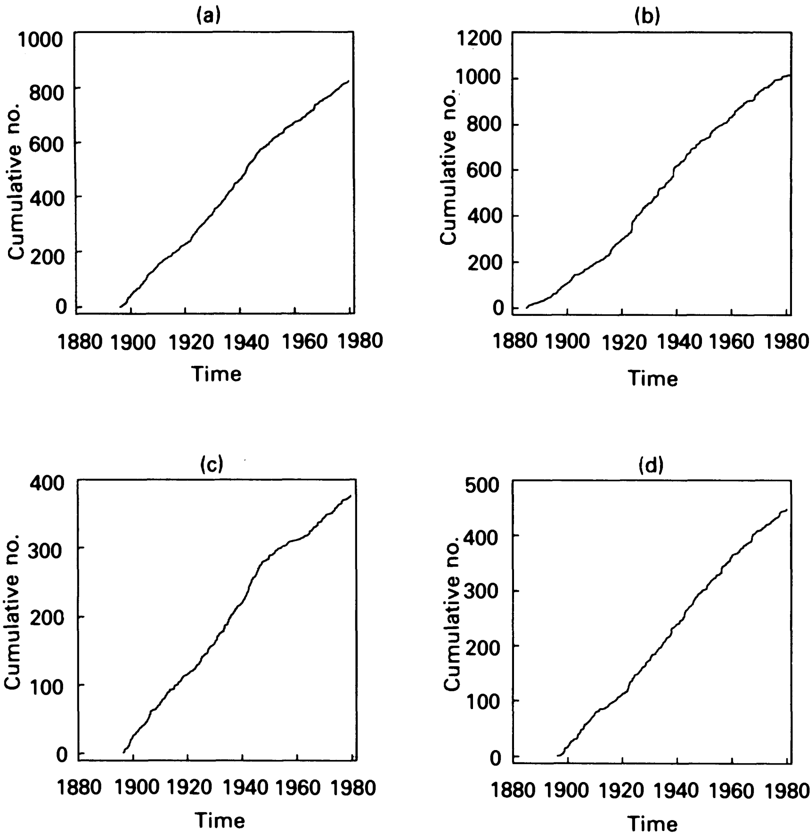

Figure 1. *Cumulative number of shallow earthquakes* (a) *with* $M_S \geq 7$ *in the world for the period* 1897–1980; (b) *with* $M_J \geq 6$ *in the regional area around Japan for* 1885–1980; (c) $M_S \geq 7$ *in low latitude area,* $|\theta| \leq 20°$, *of the world for the period* 1897–1980; (d) *and* $M_S \geq 7$ *in high latitude area,* $|\theta| > 20°$, *of the world for the period* 1897–1980; *where* θ *is latitude.*

occurrence rate is attributed to the bending cumulative curves of Figs. 1(b), (d) in the latter part of the century. It is to be noted that the two catalogs are independently compiled from different methods and data. Therefore, the coincidence of the pattern of the cumulative numbers for Japan and its vicinity with that of the global area of high latitude strongly suggests that Figs. 1(a)–(d) reflect the genuine seismicity owing to the sporadic or intermittent activation of global tectonic plate motion, see Mogi (1974) for example, rather than the artificial magnitude shift caused by the change of prevailing seismograph types.

Still, how can we explain the contradiction between the apparent trend in Fig. 1(a) and the plausible assumption that the global process of earthquakes occurrences should be stationary? This will be discussed in § 3.

3 Long Range Dependence of Earthquake Occurrence

3.1 Self-Similar Process and Long Range Dependence

Since it has been frequently reported that a variety of geophysical records exhibit self-similarity, e.g., Mandelbrot (1983), we investigate whether or not the two long-term catalogs of earthquakes have such a property. A stochastic process $Z(t)$ with stationary increments, $X(t, t+\Delta) = Z(t+\Delta) - Z(t)$, is said to be self-similar with a similarity index H $(0 < H \leqslant 1)$, if any joint distribution of the process $Z(at)$ is equal to the corresponding distribution of the process $a^H Z(t)$, for example, Mandelbrot (1983).

The long range dependence of a stochastic process is closely related to self-similarity of the process. A self-similar process with the index $\frac{1}{2} < H < 1$ has the positive auto-covariance $c(\tau)$ at time lag τ decaying to zero with the inverse power order (see (A1) in Appendix 1) as τ increases so that

$$\int_0^\infty |c(\tau)|\, d\tau = \infty$$

is said to have *long range dependence.* A process $\{Z(t)\}$ of nearly independent increments with the auto-covariance satisfying $\int |c(\tau)|\, d\tau < \infty$, where the integral is over $(0, \infty)$, is said to have the *short range dependence,* and this is approximated by the self-similar process with index $H = \frac{1}{2}$ in the sense that the process $\{Z(\sigma T)/\sqrt{T}\}$ weakly converges to the Brownian motion $\{B(\sigma)\}$ as T increases (Billingsley, 1968, p. 253). The process $\{Z(t)\}$ of the long range dependence, on the other hand, is well approximated by a self-similar process with $\frac{1}{2} < H < 1$ in the sense that the process $\{Z(\sigma T)/T^H\}$ weakly converges to a self-similar process $\{B_H(\sigma)\}$ of the index H as T increases, e.g. Taqqu (1975).

There is no rigorous process of the self-similarity among ordinary point processes with the finite first and second moments, but we can consider the approximately self-similar process in the above sense which satisfies the self-similarity in some wide finite range of frequency domain or time domain of scales. In this paper we interpret the self-similarity in such a broad sense. Kagan & Knopoff (1978, 1980) discuss the stochastic self-similarities of earthquake occurrence not only in time series but also in space. Ogata (1987) analyzed time series of earthquakes in the Seismological Bulletins of Japan Meteorological Agency and found that their occurrence possesses the self-similar property in a number of local regions. The data used in these studies were for shorter time spans and for the shocks of smaller magnitudes. Here we investigate whether the same property holds for large earthquakes over global space and long time span of 100 years.

3.2 Time Series of Events

The estimate of auto-covariances $c(\tau)$ versus time lags τ for the two data sets of the world and Japan are plotted in Figs. 2(a) and 2(b), and the *dispersion* indices versus time diagram on doubly logarithmic scales are given in Figs. 3(a) and 3(b) (see Appendix 1 for the definitions and the estimation methods). Figure 2 shows existence of significant correlations for long ranged time lags. The decreasing linearity of the dispersion-time diagrams in the time span between a few tens and some thousands days with slope $\xi = -0{\cdot}4$ $(> -0{\cdot}5)$ in both Figs. 3(a) and 3(b) relates the inverse power decay of the auto-covariances, such that $c(\tau) \doteqdot \text{const} \times \tau^\nu$ with $\nu = \xi/2$ (see Appendix 1). Indeed, when $c(\tau)$ versus time lags τ diagrams in Figs. 2(a) and 2(b) is plotted in the doubly logarithmic scale, then these are tightly aligned along a straight line, whose slope is nearly $-0{\cdot}8$, for a range from an hour up to some hundreds days: for the larger τ, however, log–log plots of the auto-covariance exhibit observation noise which surpasses the signal. Consequently we get $\hat{\nu} = -0{\cdot}8$ for both the world and Japan. On the other hand, it is known in the original and modified Omori's law for aftershock frequency that the decreasing power p of the lapse time τ empirically satisfies $p \leqslant -1$ in the most cases, e.g. Utsu (1972), Vere-Jones & Davies (1966). This implies that the present decaying rate of the auto-covariance cannot be explained in terms of the Poisson cluster process, called the trigger model, for main shock–aftershock sequences with the (modified) Omori's

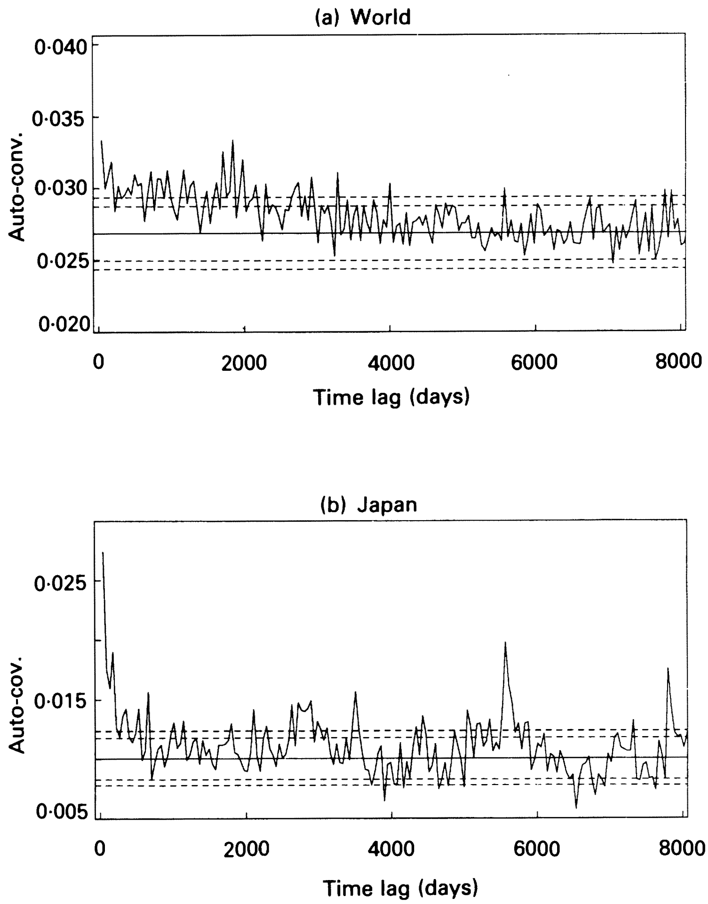

Figure 2. *Auto-covariance of occurrence times of earthquakes versus time lags* (a) *in the world for earthquakes with* $M_S \geqslant 7{\cdot}0$, *and* (b) *in and around Japan for earthquakes with* $M_J \geqslant 6{\cdot}5$. *Solid line, mean occurrence rate; dotted lines,* 95·5% *and* 99·7% *error bounds for individual estimates under the assumption of the stationary Poisson process.*

decaying law. The same matter at issue is discussed in Ogata (1987, 1988) using other Japanese earthquake occurrence data.

An auto-covariance is theoretically related to a spectrum. Therefore the so-called periodograms, or the estimated spectra are calculated for the time series of events from the two catalogs. The data were Fourier transformed into the periodograms over a wide range of $[f_{\min}, f_{\max}] = [1{\cdot}0 \times 10^{-4}, 1{\cdot}0 \times 10^{-1}]$ days^{-1} for the Abe's catalog and $[f_{\min}, f_{\max}] = [0{\cdot}5 \times 10^{-4}, 1{\cdot}0 \times 10^{-1}]$ days^{-1} for the Utsu's catalog. Assuming $\Phi(f) = cf^{\theta}$ for the spectral form, we have a likelihood of the parameters c and θ for the periodogram data to get estimates of θ and their standard errors (see Appendix 2). We obtain the maximum likelihood estimates, $\hat{\theta} = -0{\cdot}16 \pm 0{\cdot}04$ (one-fold standard error) for the occurrence of the global events, and $\hat{\theta} = -0{\cdot}25 \pm 0{\cdot}04$ (one-fold standard error) for the occurrence of the regional events of Japan. Thus the spectra of both areas seem to decrease slowly with an increase of frequency. This feature is called a $1/f$ noise, indicating the long range dependence of occurrence (Mandelbrot, 1983). These estimated values are consistent with the previous estimates of v because they satisfy the theoretical relation

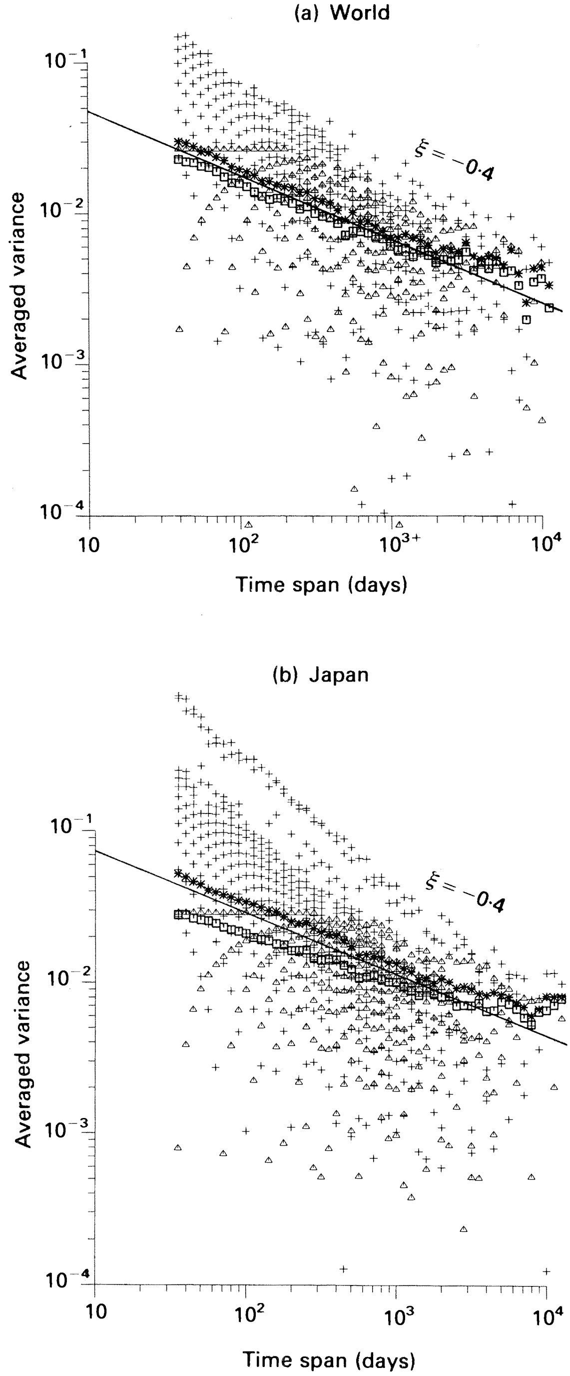

Figure 3. *Dispersions-time diagrams of time series of earthquakes* (a) *the world, and* (b) *Japan, on doubly logarithmic scales. Signs '□' and '*' for estimates of the two dispersion-time curves are tightly aligned along a straight line for a wide time span from a few tens up to some thousands days, the slope ξ of which estimates $H-1$ with self-similarity index H. See Appendix 1 for the method of estimation and for the definition of signs in the figures.*

$\nu = -(1+\theta)$ between the power ν of the decaying rate of the auto-covariance of a self-similar process and the power θ of its $1/f$ spectrum. Using the likelihood $L(c, \theta)$ in Appendix 2, we can further examine the likelihood ratio test statistic $\hat{\Lambda} = (-2)\log\{L(\hat{c}, \hat{\theta})/L(\hat{c}_0, 0)\}$ against the null hypothesis of a constant spectrum in the above frequency bands. This test ($\hat{\Lambda} = 36{\cdot}8$ and $104{\cdot}1$ for the world's and Japanese data, respectively) shows that the null hypothesis is rejected with the very high significance against the chi-square distribution with unit degree of freedom.

The R/S analysis is an estimation method proposed by Hurst (1951) and developed by Mandelbrot & Wallis (1969a, b, c), for example. This analysis examines the self-similarity and estimates the index H (*Hurst number*: see Appendix 3). Figures 4(a) and 4(b), called *Pox diagrams* (see Appendix 3), show the linear trend and its variability for the two time series of earthquake occurrence. The slope of the Pox diagram provides an estimate of H. By the least squares estimation of the linear regression, we obtain the values of $H = 0{\cdot}58$ and $0{\cdot}61$ for the world and Japan, respectively.

Finally, since the relations between the Hurst number and the parameters previously obtained are theoretically given by $\theta = 1-2H$, $\xi = H-1$ and $\nu = 2H-2$ for $0 < H \leqslant 1$ under the assumption of the self-similarity, it is noted that all the estimates obtained from the different methods are mutually consistent for each data set. This ensures that the self-similarity is satisfied in the considerable wide range of time scale for the two sets of the world and regional earthquakes.

3.3 *Some Simulation Studies*

One may suspect that the artificial trend of the non-stationary Poisson process which originates from the heterogeneity of catalogs can affect the spectrum at low frequencies, and therefore that the seismicity is likely to show seemingly long-range correlated features. Therefore, featuring the similar observation to the Table 1 in Pérez & Scholz (1984), we simulate a non-stationary Poisson process with piecewise constant rates; see Lewis & Shedler (1979) and Ogata (1981) for the method: the rates are taken by 9·3 events/year for 1897–1922, 12·9 events/year for 1923–1948, and 8·0 events/year for 1949–1980, respectively. The same simulations are carried out 99 times, and then R/S plots are made for each simulation. The short bar symbols in Fig. 5 represent the average of R/S for each length d of the time interval in each simulation: these averages are the same as those represented by the square box symbols in Fig. 4. The thicker solid lines in the figures denote the R/S averages for the world earthquake occurrence. These figures suggest that the R/S averages of the real data significantly deviate, on the time range between a few hundreds and a few thousands days, from those which are statistically expected from the nonstationary Poisson process with the adjusted piecewise constant rates.

A typical example of the self-similar stationary process is the fractional Brownian motion, fBm; see Mandelbrot (1983) for example. An approximation for the standardized fBm process with $0{\cdot}5 < H < 1$ is given by the moving average

$$X_t = (H-0{\cdot}5)\sum_{u=t-M}^{t-1}(t-u)^{H-0{\cdot}5}\xi_u,$$

where ξ_u is a sequence of independent Gaussian random variables of zero mean and unit variance, and M, called memory of the process, is taken to be sufficiently large. Here, the variable $\{X_t\}$ approximates the stationary increments $\{X(t, t+\Delta)\}$ which is given in § 3.1 (see Appendix 1 also). A sample of 10 000 values of the simulated process is provided in Mandlebrot & Wallis (1969b), from which we see stationarity, apparent cycles and extraordinarily long runs above or below the theoretical mean. In Fig. 6(a), part of the

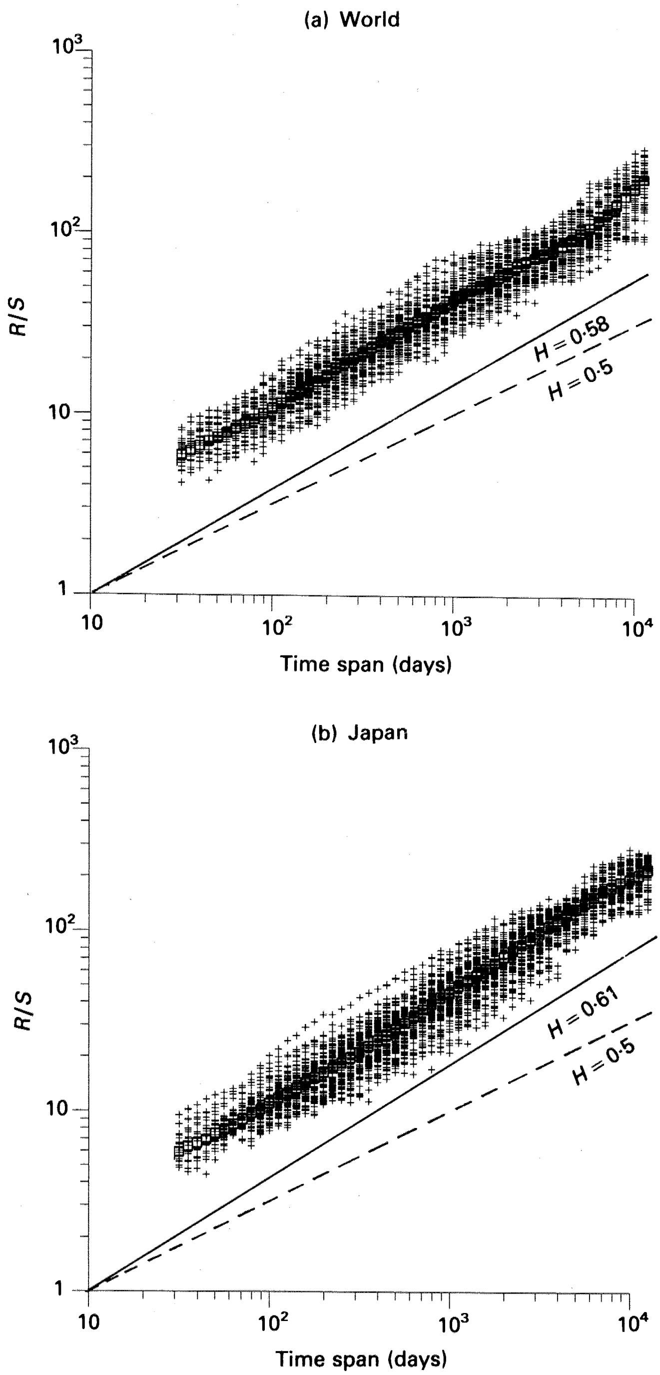

Figure 4. *Pox diagram of R/S versus time span d for the occurrence times of shallow earthquakes of* (a) *the world, and* (b) *Japan. Plus signs represent values of R/S statistic for every sampled time span of length d, and small square boxes represent their mean for each d.*

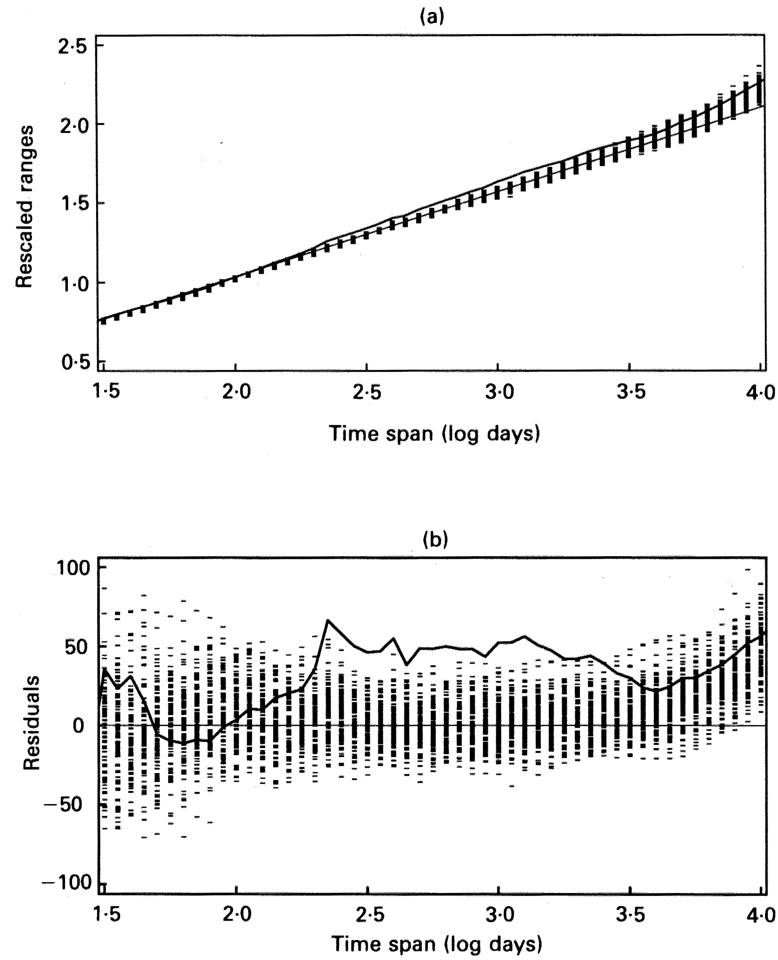

Figure 5. (a) *Pox diagram of* $\log R/S$ *versus* $\log d$: *thicker solid line represents the mean of* R/S *for each* d *(the same as the line connecting the small square boxes in Fig.* 4(a)), *minus signs represent the similar means for each of* 99 *simulations of the nonstationary Poisson process with piecewise constant occurrence rates as described in the text. Straight line, theoretical mean of* R/S *for the stationary Poisson process with the same occurrence rate as that of the world earthquakes throughout the whole time span.* (b) *Diagram of magnified residuals of the above means of* R/S *from the theoretical* R_0/S_0 *of the stationary Poisson process: that is, plot of* $10\,000\{\bar{R}(d)/\bar{S}(d) - R_0(d)/S_0(d)\}/d$ *versus* $\log d$ *for every* d. *The signs in the diagram are the same as in* (a).

similar sample is provided with $H = 0{\cdot}6$ (which is about the same as the index of the world earthquake occurrence). By a non-linear transformation, say $f(x) = e^{x/2}$, the process $\lambda_t = f(X_t)$ gets positive values (see Fig. 6(b)). Based on the process λ_t, the doubly stochastic Poisson process is simulated by the thinning method (Ogata, 1981). The histogram of the simulated points and the cumulative number versus time plot are shown in Figs. 6(c) and 6(d) respectively. This doubly stochastic Poisson process is stationary, and its spectra or auto-correlations are known to be the same as those of λ_t (Cox & Lewis (1966, p. 180) for example). The cumulative curve in Fig. 6(c) seems to be approximated by three straight lines, the middle part being steeper than the other parts. Thus, it is indicated that the apparent trend as is pointed by Pérez & Scholz (1984) can be generated by a stationary process with long range dependence.

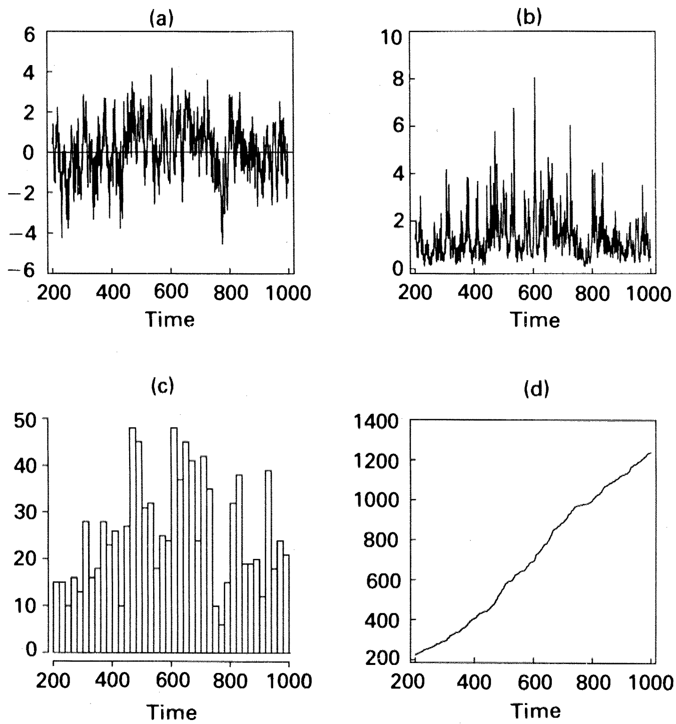

Figure 6. *(a) Part of samples from the fractional Brownian motion $\{X_t\}$ with $H = 0{\cdot}6$.* (b) *Corresponding samples $\{\lambda_t\}$ by the transformation $\lambda_t = \exp(0{\cdot}5X_t)$.* (c) *Histogram and* (d) *cumulative number of the events of the doubly stochastic Poisson process with occurrence rate $\{\lambda_t\}$.*

3.4 Limitations in Use of Z-Statistic

Pérez & Scholz (1984) used the normal deviate test (Z test) to determine whether the change of the occurrence rate in 1922 and 1948 is statistically significant at the level of 99%. The Z-statistic was extensively used for finding the significant change of apparent or real seismic activity by Habermann (e.g. Habermann, (1983)). The times of the most significant changes in occurrence rate were selected from a series of trial comparisons, in each of which the mean occurrence rate was compared for the groups of events before and after a particular event. The beginning of the first group was also fixed at the time of the first event in the data set, and the end of the second group was also fixed at the time of the last event in the data set. The boundary between the two groups (i.e., the suspected change point) was moved through the data one event at a time. The Z value is calculated for each position of the boundary

$$Z = \frac{M_1 - M_2}{\{(S_1^2/N_1) + (S_2^2/N_2)\}^{\frac{1}{2}}},$$

where M_1, M_2 are the mean occurrence rates for groups 1 and 2, S_1, S_2 are the sample standard deviations for groups 1 and 2, and N_1, N_2 are the numbers of events in groups 1 and 2. The significant per cent point is eventually calculated assuming that two samples are normally distributed with the same mean and variance. Thus $Z = \pm 2{\cdot}57$ is used for the 99% confidence level.

However, this use is criticized from two aspects. Firstly, the problem belongs to the so-called testing for change points. In the i.i.d. case of short range dependence, there is a large literature on how to choose approximately correct critical values in the Z-test or, generally, the likelihood ratios, e.g. Hinkley (1970), Shaban (1980) and Picard (1985). In the particular applications to seismic activity, Matthews & Reasenberg (1987) criticized that the significance associated with maximum or minimum of Z in searching the boundary of changing semismicity is different from the standard normal distribution described above. The difference exists because Z as a function of boundary time t searches all possible values of the maximum or minimum, rather than selecting one at random. Habermann & Craig (1988) therefore made a simulation study to get the frequency distribution of the maximum of the Z values. It was then found that the levels of 95% and 99%, for example, get remarkably higher than those of the standard case, respectively.

Secondly, we should like to note a further important point that, in the case where the samples have the long range correlation property, the significance level of the Z-statistic can be seriously higher than in the case of independent or short range dependent samples. Let $\{x_i\}$ and $\{y_i\}$ be two sets of samples from the long range correlated process with the similarity index H such that $0{\cdot}5 < H < 1$. For simplicity, assume that the theoretical mean and variance of the process are 0 and σ^2, respectively, and also that the two sample sizes are equal to each other, that is $N = N_1 = N_2$. Then consider

$$M_1 = \frac{1}{N}\sum_{i=1}^{N} x_i, \quad M_2 = \frac{1}{N}\sum_{i=1}^{N} y_i, \quad S_1^2 = \frac{1}{N}\sum_{i=1}^{n} (x_i - M_1)^2, \quad S_2^2 = \frac{1}{N}\sum_{i=1}^{N} (y_i - M_2)^2.$$

By some general conditions such as ergodicity and stationarity of the process, S_1^2 and S_2^2 are known to converge to the theoretical variance σ^2. On the other hand, by the (non) central limit theorem, e.g. Taqqu (1975), it is also known that

$$N^{-H}\sum_{i=1}^{N} x_i/\sigma, \quad N^{-H}\sum_{i=1}^{N} y_i/\sigma$$

converge in law to the distribution of some random variables ξ_0 and η_0. Based on these, for the large samples, the Z-statistic is approximately equal to

$$Z = N^{H-0{\cdot}5}(\xi_0 - \eta_0)/\sqrt{2}.$$

Note here that, if the samples are from the standard short range dependent process, then $H = 0{\cdot}5$ and ξ_0 and η_0 are mutually independent, so that the Z is the standard normal random variable. This reduces to the case where the standard significance level of the test holds. However, in case of the long term dependent process such that $0{\cdot}5 < H < 1$, ξ_0 and η_0 usually have some correlation with each other, the distribution of ξ_0 and η_0 depends on the original process, and the above Z-statistic is in particular significantly dependent on the sample size N. This suggests that the use of the Z-statistic should be carefully checked when the sample does not obey the standard short range correlations.

After all, with the consideration of the two points stated above, the high Z-values reported by Pérez & Scholz (1984) could not be suggestive of a significant change of the occurrence rate. On the contrary, this can be statistical fluctuations of a stationary process like the one shown in Fig. 6(d) in the simulation of the doubly stochastic Poisson process with the long range dependence.

3.5 *Effect of 'Removal of Aftershocks'*

There are a number of techniques which have been used for removing aftershocks from an earthquake catalog. Here, we are interested in the question whether such techniques can sufficiently exclude the dependency from the original series of earthquake occurrence.

Following the technique used by Pérez & Scholz (1984), we first filter out aftershocks from the Abe's catalog. Here we have used the moment magnitude M_w for some largest earthquakes which are given in Kanamori (1977). For the largest earthquakes ($M_S \geqslant 7{\cdot}8$ or $M_w \geqslant 7{\cdot}8$), their rupture zones are estimated by one year to a few weeks of aftershock data, depending on the size of the main event. The size is defined by a circle of radius $2r$, where r is determined from the relation $\log_{10} r = 0{\cdot}5M_w - 2{\cdot}25$ of Abe (1975). Then, we delete all the seismic events located in the rupture zone during a period of time after the main shock proportional to the size of the event: from about 6 months for $M_w = 9$ to about 1 month for $M_S = 7{\cdot}8$. For smaller main shocks, we sort out those events which occurred very close ($\leqslant$ about 100 km) to the principal epicenter, within a time span of a few days after the main event by visually inspecting the catalog. By applying this procedure sequentially in time, we have a number of clusters whose forefronts are not the largest in magnitude. Thus we may identify the largest one in the cluster as the main shock, those before the main shock as foreshocks. The total number of main shocks at the $M_S \geqslant 7$ level account for a little more than 90% of the total data set listed in Abe (1984) for the period 1897–1980.

Figure 7(a) plots the auto-covariance of such data of the main shocks. In comparison with Fig. 2(a), it seems not only that 'this aftershock removal itself has little effect on the calculated seismicity rate' as Pérez & Scholz stated, but also that the removal has little effect on the auto-correlation property. In particular, the long term dependence does seem still to exist.

Now, the problem is the magnitude shift of 0·2 in the Abe's catalog for the term from 1908 through 1948 as was claimed by Pérez & Scholz (1984). It should be noted that for the early period 1905 to 1908 the Abe's catalog was completely revised and further extended to the year 1897 by Abe & Noguchi (1983b), but this revised catalog was not used by Pérez & Scholz (1984). Taking account of this, we make a data in accordance with the claim of Pérez & Scholz. Figure 7(b) plots the auto-covariance of such an obtained data set for the earthquakes with $M_S \geqslant 7{\cdot}0$. We can see from this figure that the auto-covariance is still quite far from that expected from the stationary Poisson process: for instance, significant correlations are shown around the five to six years' time lag. In particular, the consistent bias to the negative correlation for the long time lag of 10 to 20 years may indicate that the claim of the 0·2 magnitude shift for 1908–1948 seems to be on the contrary, somewhat uncertain. Furthermore, in Fig. 8(a), the data is tested against the stationary Poisson process, using the averages of the R/S, similarly to Fig. 5(b). The graph in Fig. 8(a) indicates the significant discrepancy from that expected from the stationary Poisson process for the longer time spans of d, particularly from one to ten years.

In the Utsu's catalog of Japan and its vicinity, individual earthquakes have been classified as either main shocks, foreshocks or aftershocks, on the basis of his experienced knowledge of the seismicity in and around Japan, though the result of this classification has not been described in Utsu (1982b). Here we use this unpublished catalog (Utsu, 1988, personal communications). Figure 7(c) shows the auto-covariance for the series of the main shocks with $M_J \geqslant 6{\cdot}5$. It is still seen that the time series of the events possesses long range dependence. Although the strong dependence within a year remarkably reduces (see Fig. 2(b) for comparison), the consistent bias to the positive correlation still remains for the long time span.

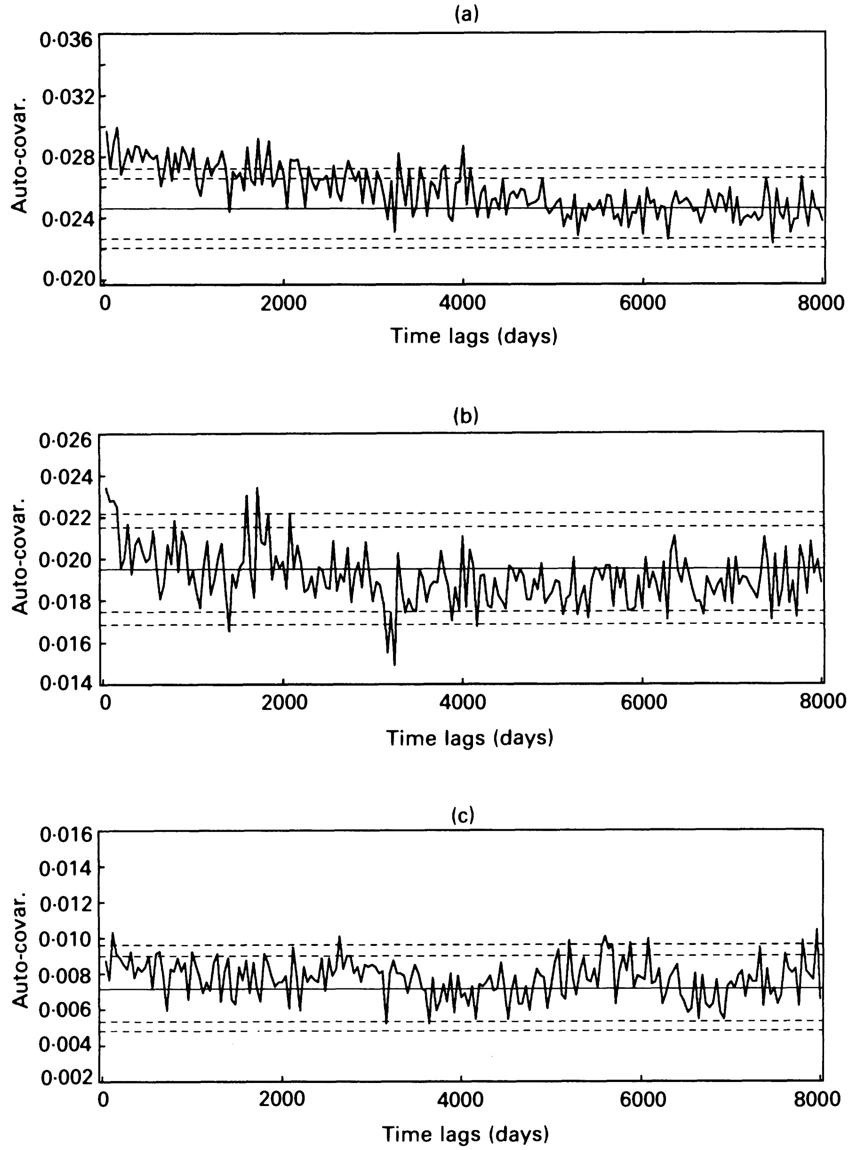

Figure 7. *Auto-covariances of the occurrence times* (a) *in the world for the main shocks with* $M_S \geqslant 7{\cdot}0$; (b) *in the world for the main shocks with* $M_{PS} \geqslant 7{\cdot}0$ *where* M_{PS} *is the magnitude shifted from* M_S *by* $-0{\cdot}2$ *for the period* 1908–1948, *otherwise* $M_{PS} = M_S$, *according to Pérez & Scholz* (1984); *and* (c) *in vicinity of Japan for the main shocks with* $M_J \geqslant 6{\cdot}5$. *Straight line, mean occurrence rate; dotted lines* 95·5% *and* 99·7% *error bounds for individual estimates under the assumption of the stationary Poisson process.*

It should be noted here that the apparent trend of the Utsu's main shock occurrence still remains, and that the cumulative curve is similar to the one seen in Fig. 1(b). If one assumes that main shocks should take place independently of each other, the occurrence times of the main shocks thus obtained must be a non-stationary Poisson process: the occurrence rate $\lambda(t)$ is a function of time t only, where t is the lapse in days from the beginning of the catalog. Having prepared the family of the functions such that

$$\lambda(t) = \exp\left\{\sum_{k=1}^{K} a_k t^{k-1}\right\},$$

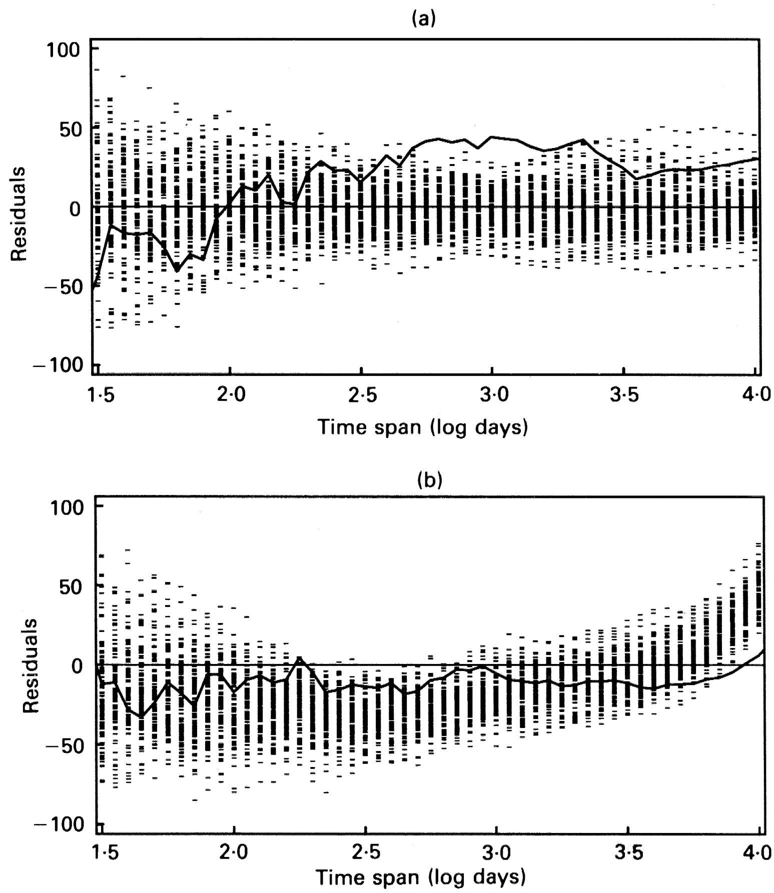

Figure 8. *Diagrams of magnified residuals of the R/S averages from the theoretical one (straight line in Fig.* 5(a)) *for the stationary Poisson process. Thicker solid lines represent the R/S average residual for each d of the earthquake data compared with those (represented by the minus signs) of 99 simulated Poisson samples: that is,* (a) *main shocks* ($M_{PS} \geq 7{\cdot}0$; *these magnitudes are altered in the same way as in Fig.* 7(b)) *of the world catalog are compared with the stationary Poisson process of the same mean rate; and* (b) *main shocks* ($M_J \geq 6{\cdot}0$) *of the Japan catalog are compared with the non-stationary Poisson process of the occurrence rate* $\hat{\lambda}(t) = \exp\{-4{\cdot}6100 + 9{\cdot}5837 \times 10^{-4}t - 2{\cdot}7758 \times 10^{-8}t^2\}$ *shocks/day, respectively.*

where $K = 1, 2, \ldots, 20$, to be fit to the present data, we found that the best fitted estimation among the family is

$$\hat{\lambda}(t) = \exp\{-4{\cdot}6100 + 9{\cdot}5837 \times 10^{-4}t - 2{\cdot}7758 \times 10^{-8}t^2\}(\text{shocks/day}),$$

according to the minimum AIC procedure (Akaike, 1974): the program EPTREN in the Fortran package TIMSAC-84 (Akaike et al., 1984) performs the selection and the maximum likelihood estimation of the exponential polynomial intensity model.

The integral

$$\int_0^t \hat{\lambda}(s)\, ds$$

as a function of t is, of course, very synchronous to the S-shaped cumulative curve of the main shocks. This is similar to Fig. 1(b), though this is not shown here. Then, using this estimated rate function, 99 sets of the data are simulated by a thinning method (Lewis & Shedler, 1979; Ogata, 1981) to compare with the Utsu's main shock data. The R/S residuals of the main shock data in Fig. 8(b) have the significant discrepancies from those expected from the estimated non-stationary Poisson process in some hundreds of days span of d and also in the time span longer than five thousand days. This implication is that the main shocks thus obtained are still likely to have long term dependence.

It is concluded here that a complete removal of the long term dependency from earthquake catalogs is quite difficult. No definition about main, fore- and aftershocks seems to be useful to remove the dependency completely from any seismic data, even if they include only large earthquakes in the very wide area such as the whole world.

3.6 *Series of Magnitudes and b-Values*

We are also interested in the sequence of the magnitudes $\{M_i; i = 1, 2, \ldots, N\}$: that is, neglecting the occurrence times of earthquakes, we make the same analysis as used in § 3.2 on the assumption that the events are supposed to have occurred at equi-spaced points. We first use the Pox diagrams of R/S. The results are given in Fig. 9. The diagrams are not so straight in comparison with Fig. 4, probably because of the small sample size of about 1000. However, it is still enough to suspect the long range dependence in these data sets, since the slope of the trend for each magnitude series appears to be slightly larger than 0·5 in the span where d is neither large nor small. We now examine the detailed analysis by using the periodogram.

The smoothed periodograms on doubly logarithmic scales for the two series of the magnitudes for the world and Japan are seen to be distributed around gradually decreasing trend at frequency lower than about 10^{-1} samples^{-1}. To get the estimates of θ, or the power of decreasing $1/f$ spectra, we also use the maximum spectral likelihood method (see Appendix 1). For the world earthquakes the estimate $\hat{\theta} = -0{\cdot}13 \pm 0{\cdot}11$ is obtained over the frequency band from $f_{\min} = 4{\cdot}0 \times 10^{-3}$ samples^{-1} to $f_{\max} = 2{\cdot}0 \times 10^{-1}$ samples^{-1}: in other words, this band corresponds to the cycles between 250 and 5 samples (roughly in the range of a half year to 25 years). In the similar way to § 3.2, the likelihood ratio test statistic against the null hypothesis of a constant spectrum in the above frequency band gives 3·8 which corresponds to about the 95% level of significance of the chi-square distribution with the unit degree of freedom. For the earthquakes in and around Japan, $\hat{\theta} = -0{\cdot}15 \pm 0{\cdot}14$ is obtained for the frequency band from $f_{\min} = 3{\cdot}0 \times 10^{-3}$ samples^{-1} (or per 333 samples, roughly corresponding to 33 years) to $f_{\max} = 6{\cdot}7 \times 10^{-2}$ samples^{-1} (or per 15 samples, roughly corresponding to 1·5 years). The likelihood ratio test statistic against the null hypothesis of a constant spectrum in the corresponding frequency band gives 1·9 which corresponds to about the 82% level of signficance of the chi-square distribution with the unit degree of freedom. From the above estimates of $\hat{\theta}$ and the relation $\theta = 1 - 2H$ we have respective individual estimates, $H = -0{\cdot}56 \pm 0{\cdot}05$ and $H = -0{\cdot}57 \pm 0{\cdot}07$. We can see that these estimates are consistent with the slopes of the Pox plot. From these observations it is suggested that the long-range dependent property of the magnitudes sequence may affect the temporal variation of b-values of the magnitude frequency distribution of the two data sets.

It is generally known that the number of earthquakes increases roughly by ten times as magnitude decreases by one unit (Gutenberg & Richter, 1944). This relation is expressed in the form $\log_{10} N = a - bM$, where N is the cumulative frequency, M is the magnitude, and a and b are constants. This means that the magnitudes are distributed marginally according to the exponential distribution. In Figs. 10(a), (b) and (c), the

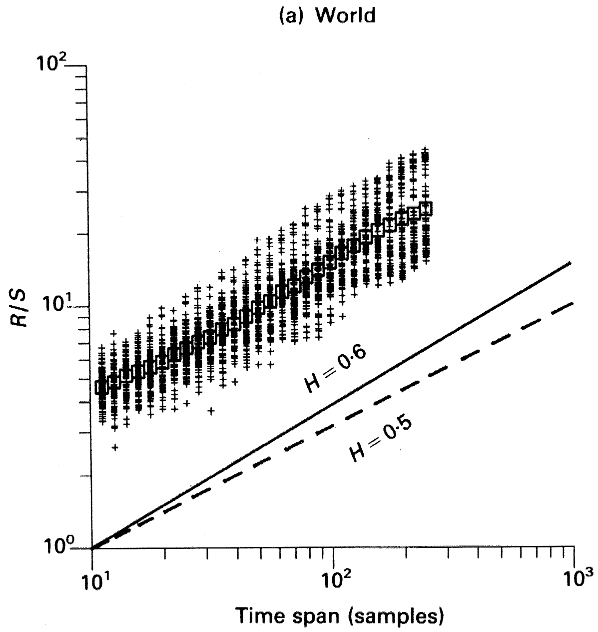

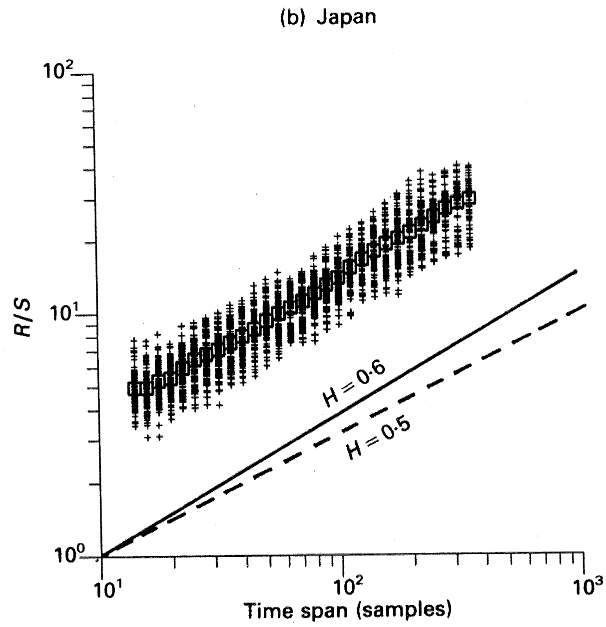

Figure 9. *Pox diagram of R/S versus span of samples d for the series of magnitudes $\{M_i\}$ of shallow earthquakes of* (a) *the world, and* (b) *Japan.*

temporal variation of the maximum likelihood estimates of b-values $\{\hat{b}_t\}$ and their error bars are plotted for the entire world, the high latitude area and the low latitude area. Here

$$\hat{b}_t = n_t \log_{10} e \bigg/ \sum_{i=1}^{n_t} (M_i - M_0),$$

where n_t is the number of earthquakes in the moving time interval centered at time t and

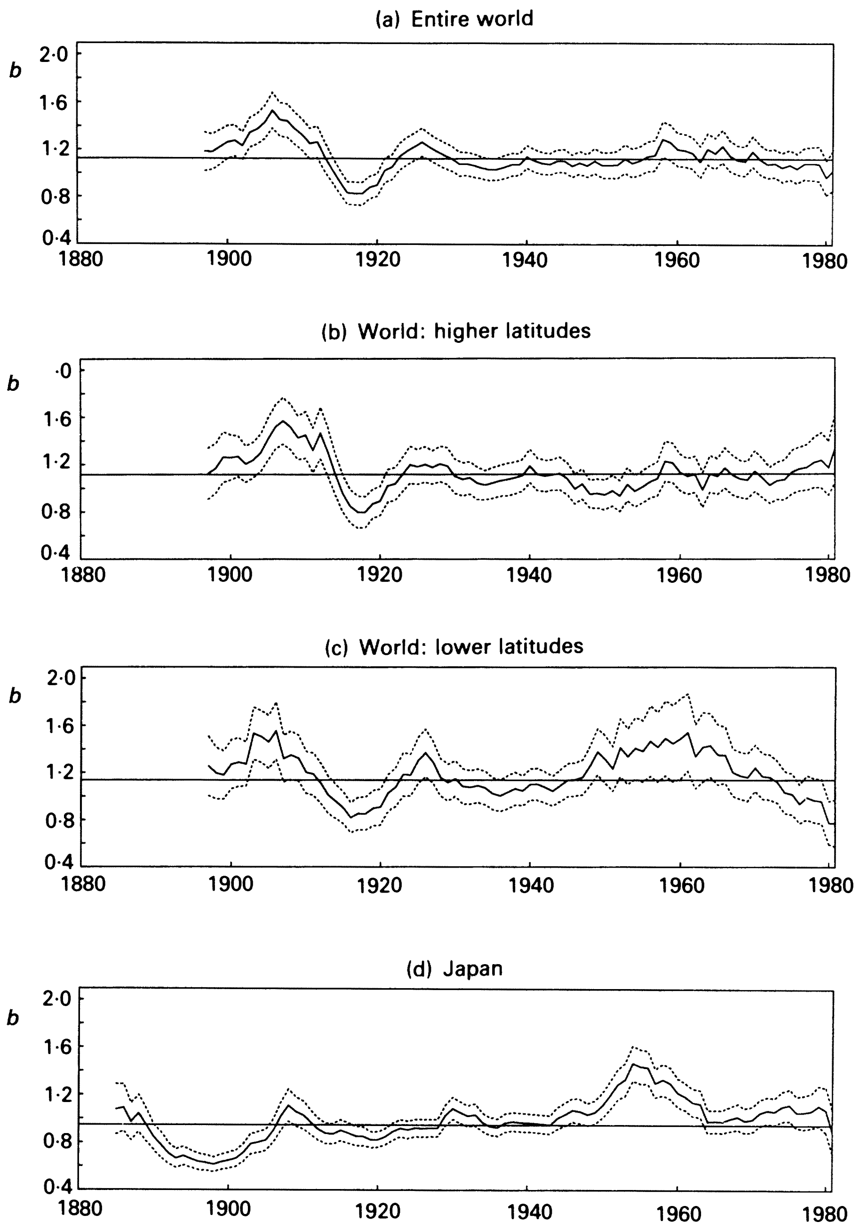

Figure 10. *Time variation of b-values of earthquakes* (a) *in the entire world,* (b) *in high latitudes of world,* (c) *low latitudes of world, and* (d) *in Japan. Solid lines show the maximum likelihood estimates for the data in the moving time intervals of* 10 *years. Dotted lines show one-fold standard errors. Straight lines represent the average over the whole period.*

M_0 is the cut-off magnitude (Utsu, 1965; Aki, 1965). The length of the moving time interval is taken to be 10 years, and $M_0 = 6{\cdot}95$. Similarly, Fig. 10(d) is obtained for the regional catalog of Japan with $M_0 = 5{\cdot}95$. It is shown that the temporal variations strongly fluctuate in b-values of the world and around Japan. This suggests that both the magnitude sequences as random variables do not seem to be identically and independently distributed. The similar feature has been suggested for an aftershock sequence of a short time span (Ogata, 1989).

4 Discussion and Conclusions

In order to measure the similarity between these two time series in Japan and the rest of the world, the cross-spectrum is calculated: to avoid the trivial coincidence, the common earthquakes that occurred in and around Japan were deleted from the Abe's catalog of the world. As a result there is no remarkable correlation in high frequencies, but a good correlation at low frequencies around $f = 1/35$ year^{-1} The corresponding phase at this low frequency is around $\theta = 0{\cdot}9$. This implies that the time delay of the two correlated components is around $\tau_{XY} = \theta(2\pi f) \simeq 5$ years. Incidentally, the coherency is close to unity around this frequency, the indication being that the correlation is almost linear about this frequency. To see the relationship in terms of time lag, the cross-correlation between the two time series was calculated for quadrennial numbers of earthquakes. The result suggests a significant correlation with time lag of 4–8 years, indicating that the change of the seismic rate in Japan apparently precedes the change in the world by some years.

The temporal variation of the earthquake frequency persistently fluctuates in the areas over the world and around Japan. In particular, the variation in the high latitude area of the world and the regional area around Japan is found to be remarkably similar to each other, in the common time period 1897–1980: the occurrence rate of earthquakes in the two areas is high in the period of 1920's to 1940 and is gradually decreasing in the last 30 years. This similarity in the two independent catalogs suggests that the catalogs reflect the change of the real seismic activity rather than the suspected heterogeneity of the world catalog. This persistent fluctuation or trend in appearance, which is very common in various geophysical records, can be understood in relation to the long range dependence, as is supported by the dispersion-time diagrams, spectrum and analysis of the R/S statistic for the occurrence times. The apparent long-term fluctuation can be reproduced by a set of samples from a stationary self-similar process.

The interpretation of the Abe's catalog by Pérez & Scholz (1984) is that the time series of the occurrence in the catalog is nearly a Poisson process with piecewise constant rates which change in 1922 and 1948. Therefore, we made a simulation study of the nonstationary Poisson process to find the signficant difference of the R/S statistic with that of the real data. Pérez & Scholz have also used the normal deviate test (Z test) for checking the difference between two means to determine whether a rate change of the seismicity is statistically significant at some level. Besides the criticism raised by Matthews & Reasenberg (1987), however, there arises another serious doubt, because of the intrinsic feature of the data, to the justification of their significance level of the Z test statistic. This significance level was given on the assumption of independence or short range dependence at most. The complete removal of dependent shocks besides aftershocks seems nearly impossible for such data with long range dependence. Eventually, implementation of the Z test procedure should be carefully checked in studies of seismicity.

Acknowledgments

We thank Koichi Katsura of the Institute of Statistical Mathematics for preparing some figures. Professor Utsu kindly informed us of his identification of the main shocks, fore- and aftershocks in his earthquake catalog. The research of Y. Ogata was undertaken while he was a guest research associate of the Earthquake Research Institute, University of Tokyo.

Appendix 1 Auto-Covariance and Dispersion-Time Diagrams

Consider a stationary increment $X(t, t+\Delta) = Z(t+\Delta) - Z(t)$ of the cumulative process $Z(t)$. If the process $Z(t)$ is self-similar, the auto-covariance $c(\tau)$, for not too small a time lag $\tau > 0$, satisfies the relation (Mandelbrot, 1983)

$$\begin{aligned} c(\tau)\,d\tau\,dt &= \mathrm{Cov}\,\{X(t, t+dt); X(t+\tau, t+\tau+d\tau)\} \\ &\propto H(2H-1)\tau^{2H-2}\,d\tau\,dt, \end{aligned} \tag{A1}$$

for some H ($\frac{1}{2} < H \leq 1$). For the stationary point processes with finite second moments, only approximations of self-similar processes exist in some wide finite range of time domain or frequency domain. They possess the long range dependence property with the above relation (A1) for sufficiently large τ. Write

$$V(\tau) = \mathrm{Var}\,\{N(t, t+\tau)\}, \quad \lambda = E[N(t, t+\tau)/\tau]$$

for the variance function and the intensity rate of the weakly stationary point process, respectively, where $N(t, t+\tau)$ denotes the number of points (events) in the interval $(t, t+\tau)$. Since $c(\tau) = V''(\tau)/2$ ($\tau \neq 0$) holds under very regular conditions (Daley, 1971), it is expected to satisfy that $\sqrt{V(\tau)}/(\lambda\tau) \propto \tau^{H-1}$. It is also expected by the (non) central limit theorem (see § 3.4) that $E\,|N(t, t+\tau) - \lambda\tau|/(\lambda\tau) \propto \tau^{H-1}$. We call these functions *dispersion-time curves* in this paper.

To draw the dispersion-time diagrams on doubly logarithmic paper, define

$$B(t_j; \tau_k) = \{N(t_j, t_j + \tau_k) - \hat{\lambda}\tau_k\}/(\hat{\lambda}\tau_k)$$

with $\hat{\lambda} = N(0, T)/T$, and select a sequence of lags $\{\tau_k\}$ in such a way that the lengths $\{\tau_{k+1} - \tau_k\}$ of the subintervals are taken to increase geometrically, say $\tau_k = 10^{k/10}$ for $k = -30, -29, \ldots, 39, 40$ (plotted as the abscissas). Then, dots of $|B(t_j; \tau_k)|$ versus τ_k are plotted for a number of equidistantly sampled $\{t_j\}$ from the first three quarters, say, of the observation time interval $[0, T]$: in Figs. 3(a) and 3(b), + signs are marked if the $B(t_j; \tau_k)$ is positive, otherwise Δ signs are marked. Finally, for each τ_k the sample average of $|B(t_j; \tau_k)|$ with respect to t_j's is marked by a little square box as an estimate of $E\,|N(t, t+\tau_k) - \lambda\tau_k|/(\lambda\tau_k)$, while the standard deviation of $B(t_j; \tau_k)$ with respect to t_j's is marked by '*' as an estimate of $\sqrt{V(\tau_k)}/(\lambda\tau_k)$. We examine whether '□' and '*' are tightly aligned along a straight line, the slope ξ of which will be equal to $H-1$, which are expected to be affirmative in case of the self-similar record. The value $\xi = -0{\cdot}5$ has a special significance, since it suggests short range dependence. On the other hand $-0{\cdot}5 < \xi < 0$ suggests long range dependence of the process. It should be noted here that the present plots of the $B(t_j; \tau_k)$ for the longer time spans τ_k's are dominated by the effect of the (non) central limit theorem as described in § 3.4.

Appendix 2 Spectral Likelihood to Estimate $1/f$-Spectrum

Suppose marked point process data $\{(t_j, X)_i\}$ is observed on time interval $[0, T]$, where t_j is the occurrence time of a jump with the jump size (scalar of the mark) $X_j = Z(t_j) - Z(t_j-)$, of a cumulative process $\{Z(t)\}$. The estimate of the spectrum, or periodogram, for a marked point process is defined by

$$I(f) = \frac{1}{2\pi T}\left|\sum_{j=1}^{J} X_j e^{2\pi i t_j f}\right|^2 = \frac{1}{2\pi T}[C^2(f) + S^2(f)], \tag{A2}$$

where f is a frequency, and where

$$C(f) = \sum_{j=1}^{J} X_j \cos(2\pi t_j f), \quad S(f) = \sum_{j=1}^{J} X_j \sin(2\pi t_j f)$$

(see Cox & Lewis (1966, p. 126) for example).

Consider the spectrum model of the form $\Phi(f \mid c, \theta) = cf^{\theta}$ for a frequency band $f_{\min} \leqslant f \leqslant f_{\max}$. As the periodogram $I(f_p)$ for a frequency f_p should show an asymptotically exponential distribution with the average $\Phi(f_p \mid c, \theta)$, it seems reasonable to use the approximate log-likelihood (see Hawkes & Adamopoulos (1973), and also Künsch (1986) for the ordinary time series)

$$\log L(c, \theta) = -\sum_{\{p: f_{\min} \leqslant f_p \leqslant f_{\max}\}} \left[\log \Phi(f_p \mid c, \theta) + \frac{I(f_p)}{\Phi(f_p \mid c, \theta)}\right], \tag{A3}$$

where $\{f_p\}$ is equidistantly sampled from the frequency band $[f_{\min}, f_{\max}]$.

Maximizing this function we can numerically get the estimates of c and θ. The standard errors are obtained from the inverse Hessian of the above function: that is, for the estimate of $(\hat{c}, \hat{\theta})$, the Normal distribution $N(0, J(\hat{c}, \hat{\theta})^{-1})$ is expected for the errors, where $J(c, \theta) = \{J_{j,k}\}_{j,k=1,2}$ is given by

$$J_{11} \doteq -\frac{\partial^2 \log L}{\partial c^2} = \sum_{\{p: f_{\min} \leqslant f_p \leqslant f_{\max}\}} \frac{1}{c^2},$$

$$J_{12} = J_{21} \doteq -\frac{\partial^2 \log L}{\partial c\, \partial \theta} = \sum_{\{p: f_{\min} \leqslant f_p \leqslant f_{\max}\}} \frac{\log f_p}{c},$$

$$J_{22} \doteq -\frac{\partial^2 \log L}{\partial \theta^2} = \sum_{\{p: f_{\min} \leqslant f_p \leqslant f_{\max}\}} \log^2 f_p.$$

Appendix 3 *R/S* Statistic for Point Processes

The R/S statistic has been used in hydrology for the purpose of solving engineering problems of water control such as that of designing a reservoir, and was first invented by Hurst (1951) in analyzing records of stream flow of the Nile river. Here, a definition of the R/S statistic is described for point processes. Consider a step function on an arbitrary interval $(t, t+d)$ of length d for a sample configuration of a point process which jumps with a size of the mark at each occurrence time (see Fig. A1). Let $Z(t)$ be the cumulative of jump sizes at time t from the time origin. Then the deviation of the cumulative from

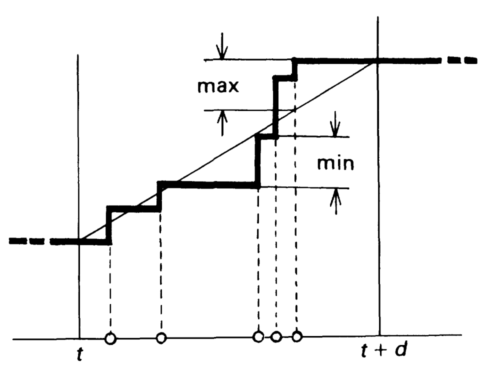

Figure A1. *Diagram showing the construction of the sample range $R(t; d)$. The function $D(\tau, t, d)$ stands for*

$$Z(t+\tau) - Z(t) - (\tau/d)[Z(t+d) - Z(t)] = X(t, t+\tau) - (\tau/d)X(t, t+d),$$

and the sample range is defined as

$$R(t; d) = \max_{0 \leqslant \tau \leqslant d} D(\tau, t, d) - \min_{0 \leqslant \tau \leqslant d} D(\tau, t, d).$$

the average increase of the step function in the interval $(t, t+d)$ is given by

$$\begin{aligned} D(\tau, t, d) &= [Z(t+\tau) - Z(t)] - (\tau/d)[Z(t+d) - Z(t)] \\ &= X(t, t+\tau) - (\tau/d)X(t, t+d), \end{aligned}$$

where $X(a, b)$ is the total length of jump sizes of events occured in the time interval (a, b). The range of extremes from the mean increase, called the *rescaled range*, is defined by

$$R(t; d) = \max_{0 \le \tau \le d} D(\tau, t, d) - \min_{0 \le \tau \le d} D(\tau, t, d). \tag{A4}$$

Further, $S(t; d)^2$ is a sample variance of the random variable $X(t, t+d) = Z(t+d) - Z(t)$, and this estimate for the marked point-process data is practically obtained by

$$S(t; d)^2 = \sum_i \frac{m_i^2}{M} - \left\{\sum_i \frac{m_i}{M}\right\}^2, \tag{A5}$$

where $\{m_i\}$ is a sequence of the total length of the marks (numbers of points for the case of simple point processes owing to the unit marks) on equally divided M subintervals of $(t, t+d)$ of the length $\Delta = d/M$. The R/S statistic is thus defined by $R(t; d)/S(t; d)$. It is shown in Mandelbrot & Wallis (1969c) that the role of the $S(t; d)$ is to stabilize the R/S statistic for the non-Gaussian time series, of course including the case of our point processes.

To construct a *Pox diagram*, a sequence of values of the lag d is selected and marked on the axis of abscissas on doubly logarithmic paper. For each d, one selects a number of equidistantly sampled starting points t_i from the first two thirds, say, of the observation time interval, and the values of $R(t_i; d)/S(t_i; d)$ so obtained are plotted as ordinates. Thus, above every marked values of d, several points (marked by + signs) are aligned. For each d, the sample average of the quantities $R(t_i; d)/S(t_i; d)$ with respect to t_i is marked by a little square box. The line connecting such boxes weaves through the Pox diagram.

An empirical record is said to satisfy *Hurst's law* if, save perhaps for very small and very large values of d, the Pox diagram of the R/S is tightly aligned along a straight line, the slope of which will be designated by H. Typically, one has $0 < H < 1$, the value $H = 0{\cdot}5$ having a special significance, because it suggests that observations sufficiently distant from each other in time are statistically independent: this is called short range dependence.

References

Abe, K. (1975). Reliable estimation of the seismic moment of large earthquakes. *J. Phys. Earth.* **23,** 381–390.

Abe, K. (1981). Magnitudes of large shallow earthquakes from 1904 to 1980. *Phys. Earth. Planet. Inter.* **27,** 72–92.

Abe, K. (1984). Complements to "Magnitudes of large shallow earthquakes from 1904 to 1980". *Phys. Earth. Planet. Inter.* **34,** 17–23.

Abe, K. & Noguchi, S. (1983a). Determination of magnitudes for large shallow earthquakes 1898–1917. *Phys. Earth. Planet. Inter.* **32,** 45–59.

Abe, K. & Noguchi, S. (1983b). Revision of magnitudes of large earthquakes 1897–1912. *Phys. Earth. Planet. Inter.* **33,** 1–11.

Akaike, H. (1974). A new look at the statistical model identification. *IEEE Trans. Autom. Control* **19,** 716–723.

Akaike, H., Ozaki, T., Ishiguro, M., Ogata, Y., Kitagawa, G., Tamura, Y.H., Arahata, E., Katsura, K. & Tamura, Y. (1984). *Time Series Analysis and Control Program Package, TIMSAC-84.* Tokyo: Institute of Statistical Mathematics.

Aki, K. (1965). Maximum likelihood estimate of b in the formula $\log N = a - bM$ and its confidence limits. *Bull. Earthq. Res. Inst., Univ. Tokyo* **43,** 237–239.

Billingsley, P. (1968). *Convergence of Probability Measures*. New York: Wiley.
Cox, D.R. & Lewis, P.A.W. (1966). *The Statistical Analysis of Series of Events*. London: Methuen.
Daley, D.J. (1971). Weakly stationary point processes and random measures. *J. R. Statist. Soc.* B **33,** 406–428.
Gutenberg, B. (1945). Amplitudes of surface waves and magnitudes of shallow earthquakes. *Bull. Seismol. Soc. Am.* **35,** 3–12.
Gutenberg, B. & Richter, C.F. (1944). Frequency of earthquakes in California. *Bull. Seismol. Soc. Am.* **34,** 185–188.
Habermann, R.E. (1983). Teleseismic detection in the Aleutian Island arc. *J. Geophys. Res.* **88,** 5056–5064.
Habermann, R.E. & Craig, M.S. (1988). Comparison of Berkeley and CALNET magnitude estimates as a means of evaluating temporal consistency of magnitudes in California. *Bull. Seismol., Soc. Am.* **78,** 1255–1266.
Hawkes, A.G. & Adamopoulos, L. (1973). Cluster models for earthquakes: regional comparisons. *Bull. Int. Statist. Inst.* **45,** 454–461.
Hayashi, Y. & Abe, K. (1984). A method of M_S determination from JMA data (in Japanese). *J. Seismol. Soc. Japan,* **37,** 429–439.
Hinkley, D.V. (1970). Inference about the change-point in a sequence of random variables. *Biometrika* **57,** 1–17.
Hurst, H.E. (1951). Long-term storage capacity of reservoirs. *Trans. Am. Soc. Civil Engineers* **116,** 770–808.
Kagan, Y.Y. & Knopoff, L. (1978). Statistical study of the occurrence of shallow earthquakes. *Geophys. J. R. Astron. Soc.* **55,** 67–86.
Kagan, Y.Y. & Knopoff, L. (1980). Spatial distribution of earthquakes: The two-point correlation function. *Geophys. J. R. Astron. Soc.* **62,** 303–320.
Kanamori, H. (1977). The energy release in great earthquakes. *J. Geophys. Res.* **82,** 2981–2987.
Künsch, H.R. (1986). Statistical aspect of self-similar processes. Research Report, No. 51, Seminar für Statistik, pp. 9. Zuerich: Eidgenoessische Technische Hochschule, also Proc. 1st World Congress of the Bernoulli Society.
Lewis, P.A.W. & Shedler, G.S. (1979). Simulation of nonhomogeneous Poisson processes by thinning. *Naval Res. Logistics Quart.* **26,** 403–413.
Mandelbrot, B.B. (1983). *The Fractal Geometry of Nature*. New York: Freeman.
Mandelbrot, B.B. & Wallis, J.R. (1969a). Some long-run properties of geophysical records. *Water Resources Res.* **5,** 321–340.
Mandelbrot, B.B. & Wallis, J.R. (1969b). Computer experiments with fractional Gaussian noises. Part 1, Averages and variances. *Water Resources Res.***5,** 228–241.
Mandelbrot, B.B. & Wallis, J.R. (1969c). Robustness of the rescaled range R/S in the measurement of noncyclic long run statistical dependence. *Water Resources Res.* **5,** 967–988.
Matthews, M.V. & Reasenberg, P. (1987). Comment on Habermann's method for detecting seismicity rate changes. *J. Geophys. Res.* **92,** 9443–9445.
Mogi, K. (1974). Active periods in the world's chief seismic belts. *Tectonophys.* **22,** 265–282.
Mogi, K. (1979). Global variation of seismsic activity. *Tectonophys.* **57,** 43–50.
Ogata, Y. (1981). On Lewis's simulation method for point processes. *IEEE Trans. Inform. Theory* **IT-30,** 23–31.
Ogata, Y. (1983). Estimation of the parameters in the modified Omori formula for aftershock frequencies by the maximum likelihood procedure. *J. Phys. Earth* **31,** 115–124.
Ogata, Y. (1987). Long term dependence of earthquake occurrences and statistical models for standard seismic activity (in Japanese). In *Suri Zisin Gaku (Mathematical Seismology) II,* Ed. M. Saito, pp. 115–124, Cooperative Research Report 3. Tokyo: Institute of Statical Mathematics.
Ogata, Y. (1988). Statistical models for earthquake occurrences and residual analysis for point processes. *J. Am. Statist. Assoc.* **83,** 401.
Ogata, Y. (1989). Statistical models for standard seismicity and detection of anomalies by residual analysis. *Tectonophys.* **169,** 159–174.
Pérez, O.J. & Scholz, C.H. (1984). Heterogeneities of the instrumental seismicity catalog (1904–1980) for strong shallow earthquakes. *Bull. Seismol. Soc. Am.* **74,** 669–686.
Picard, D. (1985). Testing and estimating change-points in time series. *Adv. Appl. Prob.* **17,** 841–867.
Shaban, S.A. (1980). Change point problem and two-phase regression: an annotated bibliography. *Int. Statist. Rev.* **48,** 83–93.
Taqqu, M. (1975). Weak convergence to fractional Brown motion and to the Rosenblatt process. *Z. Wahr. verw. Geb.* **31,** 287–302.
Tsuboi, C. (1954). Determination of the Gutenberg–Richter's magnitude of earthquakes occurring in and near Japan (in Japanese). *J. Seismol. Soc. Japan* **7,** 185–193.
Utsu, T. (1965). A method for determining the value of b in a formula $\log n = a - bM$ showing the magnitude-frequency relation for earthquakes (in Japanese). *Geophys. Bull. Hokkaido Univ.* **13,** 99–103.
Utsu, T. (1972). Aftershocks and earthquake statistics (IV)—Analyses of the distribution of earthquakes in magnitude, time and space with special consideration to clustering characteristics of earthquake occurrence (2). *J. Fac. Sci., Hokkaido Univ.*, Ser. VII (Geophysics) **4,** 1–42.
Utsu, T. (1979). Seismicity of Japan from 1885 through 1925: A new catalog of earthquakes of $M \geqslant 6$ felt in Japan and smaller earthquakes which caused damage in Japan (in Japanese). *Bull. Earthq. Res. Inst., Univ. Tokyo* **54,** 253–308.
Utsu, T. (1982a). Seismicity of Japan from 1885 through 1925: Correction and supplement (in Japanese). *Bull. Earthq. Res. Inst., Univ. Tokyo* **57,** 111–117.

Utsu, T. (1982b). Catalog of large earthquakes in the region of Japan from 1885 through 1980 (in Japanese). *Bull. Earthq. Res. Inst., Univ. Tokyo* **57**, 401–463.

Utsu, T. (1982c). Relationships between earthquake magnitude scales (in Japanese). *Bull. Earthq. Res. Inst., Univ. Tokyo* **57**, 465–497.

Vere-Jones, D. & Davies, R.B. (1966). A statistical survey of earthquakes in the main seismic region of New Zealand: part 2, Time series analysis. *N. Z. J. Geol. Geophys.* **9**, 251–284.

Résumé

On étudie la variation temporelle de l'activité sismologique donnant lieu aux tremblements de terre peu profonds dans le monde entier ainsi que dans la région du Japon en particulier. On se base sur deux catalogues de tremblements de terre: le catalogue d'Abe des tremblements de terre globals d'amplitude $M_S \geqslant 7$ durant la période de 1897 a 1980 et celui d'Utsu des tremblements de terre de la région Japonaise et d'amplitude $M_J \geqslant 6$ durant la période. Les taux de tremblements de terre sont elevés dans chaque région pour la période de 1920 a 1950 et ils sont reduits dans les trentes dernières années. La manifestation apparente de cette tendence peut être liée à la dépendance statistique à long terme de la série chronologique des tremblements de terre. On calcule pour chaque catalogue des indices mesurant l'envergure de cette dépendance. Péres et Scholz (1984) ont souligné que les catalogues étaient non-homogènes si l'on suppose que le taux de tremblements de terre global fut constant pour la durée du siecle, ce qui n'est pas garanti en vue de la dependance á long terme de la série chronologique de tremblements de terre. La variation synchronisée des frequences sismologiques des regions du monde a haute latitude avec celles de la région du Japon que l'on obtient à partir de catalogues independants suggère plutôt un effet externe tel que le mouvement de la terre sur une grande échelle.

[*Received August* 1989, *accepted October* 1990]